
Redefining Instance Matching: A Unified Framework for Part-Aware Matching in Panoptic Segmentation Evaluation

Erik Großkopf¹, Soumya Snigdha Kundu², Hendrik Möller³, Nicolas Münster¹,
Mehdi Astaraki⁴, Paula Tamara Buzduga¹, Kerstin Ritter¹, Benedikt Wiestler³,
Jan Kirschke³, Jonathan Shapey², Tom Vercauteren², Florian Kofler¹

¹Hertie Institute for AI in Brain Health, University of Tübingen, Germany

²King’s College London, UK

³Technical University of Munich, Germany

⁴Stockholm University, Sweden

Abstract

The Panoptic Quality (PQ) metric is the standard for jointly evaluating instance and semantic segmentation. However, its original definition relies on a One-to-One matching between predicted and ground truth segments, which is only straightforward when the IoU threshold exceeds 0.5. Below 0.5, multiple matching strategies emerge in a poorly explored problem space. We systematically elucidate this space by recasting segment matching as a constrained bipartite assignment problem. Independently bounding the prediction- and ground-truth-side degrees yields four matching strategies: One-to-One, Many-to-One, One-to-Many, and Many-to-Many. We show that the first three are well-defined within the PQ framework, while Many-to-Many falls outside it. These strategies become relevant when instances are fragmented, adjacent objects are difficult to delineate, or annotations are noisy. Central to our framework is a *vertex-based* accounting of TP, FN, and FP, anchored to ground truth and predicted segments rather than to matching edges. We further show that the framework extends naturally to part-aware panoptic segmentation, and we explore part-aware evaluation on biomedical data. Across configurable case studies we report how different combinations of thresholds and matching strategies behave in practice. We release a unified open-source package built on Panoptica. It exposes Voronoi-based region-wise analysis, part-aware evaluation, and Area Under Threshold Curve computations as configurable options.

Panoptic Segmentation (PS) [13] unifies semantic and instance segmentation under a single metric, *Panoptic Quality (PQ)*. *PQ* is defined through a One-to-One matching of predicted to ground truth segments at a fixed $\text{IoU} > 0.5$ threshold. The threshold makes the matching trivial: above 0.5, at most one prediction can overlap a given ground truth segment, so the assignment reduces to a lookup. Below it, the original definition is undefined. Part-aware Panoptic Segmentation [6] later extended *PQ* to hierarchical targets, where a scene-level instance carries a meaningful part decomposition, but inherited the matching rule unchanged.

Two limitations follow. First, the One-to-One rule is brittle whenever predictions and references legitimately split or merge. An instance, correctly recovered as several adjacent fragments scores as one true positive and several false positives, even if their union matches the reference well. Several recent metrics tackle parts of this problem. Examples include proximity-based per-component evaluation [11], topology-aware connected-component Dice [22], and many-to-many Cluster Dice [17]. Each one targets a single failure mode. They do not share a common framework, and none extends to hierarchical evaluation. Second, the $\text{IoU} > 0.5$ threshold is an opinionated default. A prediction with

IoU = 0.49 is treated identically to one with zero overlap, and the choice of threshold heavily shapes the resulting score. These issues bite hardest where instances are small, dense, or hierarchically organised: tiny-instance benchmarks, where a one-pixel shift dominates IoU [7], scene parsing with internal part annotations [6], and biomedical data, where lesions decompose into sub-regions and where expert disagreement induces ambiguous instance boundaries.

We address both limitations by recasting segment matching as a weighted bipartite assignment problem. Edges are formed between predicted and ground truth segments with IoU above a configurable threshold $\tau \in [0, 1)$, and TP, FP, and FN are anchored to the vertices of the resulting graph rather than to matched edges. This vertex-centric formulation preserves the invariant $|TP| + |FN| = |G|$ across all matching strategies and generalises PQ to any τ . It admits four strategies: One-to-One, Many-to-One, One-to-Many, and Many-to-Many. The first three are well-defined within the PQ framework, and each one either tolerates or penalises a specific segmentation failure mode. Many-to-Many breaks key invariants and falls outside the framework. At $\tau > 0.5$, the One-to-One case recovers the original PQ exactly. The same formalism defines the *Area under Threshold Curve (AUTC)*, the threshold-agnostic summary $\int_0^1 PQ(\tau) d\tau$, which inherits the same configurability across strategies and parts. *AUTC* decomposes into segmentation- and recognition-specific terms that isolate the source of a method’s threshold-averaged performance. For settings with dense, touching instances, we additionally describe a Voronoi-based region-wise variant. It complements One-to-Many matching by partitioning the image into per-instance cells, in which the same bipartite construction is applied locally.

As an add-on for hierarchical targets, we extend PartPQ to this framework and decouple it from the original One-to-One rule. The part-aware quality term then composes with any of our matching strategies. We release all of the above as a unified open-source package built on the Panoptica pipeline [14]. The package also exposes the prior approaches discussed above as configurable options, so practitioners can select the matcher and quality term that fits their task rather than adopting a tool’s default. We then assess the practical consequences of these choices across different case studies, including the previously unstudied interaction between matching strategy and part-level evaluation.

1 Preliminaries

Semantic segmentation assigns every pixel/voxel i a single class label $l_i \in \mathcal{L}$ [19]. Pixels/voxels are grouped only by class, so distinct instances of the same class merge into one region. Instance segmentation requires a method to delineate every object instance in an image with a binary mask, typically accompanied by a class label and a confidence score [9, 8]. Unlike *PS*, it considers only thing classes and permits overlapping masks, since each instance is predicted independently rather than as a partition of the image.

PS, introduced by Kirillov et al. [13], unifies semantic and instance segmentation into a single coherent task. Given a set of L semantic classes $\mathcal{L} = \mathcal{L}^{\text{St}} \cup \mathcal{L}^{\text{Th}}$, a *PS* algorithm assigns every pixel/voxel i a pair $(l_i, z_i) \in \mathcal{L} \times \mathbb{N}$, where l_i denotes the semantic class and z_i the instance id. *Stuff* classes (e.g. *grass*, *sky*) are amorphous regions for which the instance id is irrelevant, while *thing* classes (e.g. *sheep*, *car*) are countable objects whose pixels/voxels must be partitioned into distinct instances. Unlike instance segmentation, *PS* forbids overlapping segments by construction, so each pixel/voxel receives exactly one label pair (see visual comparison of segmentation tasks in section C).

Panoptic Quality. To evaluate *PS* on a single scale, Kirillov et al. [13] introduced the PQ metric. PQ proceeds in two steps: (i) matching predicted segments to ground truth segments, and (ii) aggregating the matches into a single score per class, which is then averaged over classes. A predicted segment p matches a ground truth segment g when their intersection-over-union $\text{IoU}(p, g) = |p \cap g| / |p \cup g|$ satisfies $\text{IoU}(p, g) > 0.5$. Together with the non-overlap property of *PS*, this threshold guarantees a *unique* matching: at most one predicted segment can match each ground truth segment, and vice versa, so no assignment problem needs to be solved [13, Theorem 1]. The matched pairs form the *True Positives (TPs)*, while unmatched predictions and ground truth segments form the *False Positives (FPs)* and *False Negatives (FNs)*, respectively. PQ is then defined as

$$PQ = \frac{\sum_{(p,g) \in TP} \text{IoU}(p, g)}{|TP| + \frac{1}{2}|FP| + \frac{1}{2}|FN|}} = \underbrace{\frac{\sum_{(p,g) \in TP} \text{IoU}(p, g)}{|TP|}}_{\text{SQ}}} \times \underbrace{\frac{|TP|}{|TP| + \frac{1}{2}|FP| + \frac{1}{2}|FN|}}_{\text{RQ}}, \quad (1)$$

which decomposes into a *segmentation quality* term SQ, the average *Intersection over Union (IoU)* of matched segments, and a *recognition quality* term RQ, equivalent to the F_1 score [24]. All segments contribute equally regardless of area.

Part-aware Panoptic Quality. De Geus et al. [6] extend *PS* with a third level of granularity: each thing instance may carry an internal decomposition into a fixed set of *parts*, e.g. a *person* into head, torso, arms, and legs. The corresponding metric, Part-aware Panoptic Quality (*PartPQ*), inherits the matching machinery of *PQ* and reweights only the per-pair quality so that parts contribute to the score only through a successfully matched parent instance. To our knowledge, PartPQ is the only existing panoptic-style metric that jointly evaluates instances and their internal parts, and it has not previously been applied to biomedical data. We revisit it formally in section 3.7 and showcase its adoption within the medical image analysis framework.

The 0.5 threshold. Kirillov et al. [13] argue that lower thresholds are unnecessary because matches with $\text{IoU} \leq 0.5$ are rare in practice. This assumption breaks down in domains where boundary localization is inherently ambiguous or where small, densely packed instances dominate the data. Biomedical imaging offers a plethora of such regimes, including multiple sclerosis lesion segmentation [15] and brain-metastasis segmentation in MR [21], liver and abdominal metastasis in CT [2, 10, 1], encapsulin segmentation in electron microscopy [23], and neuron segmentation in light-sheet microscopy [12]. In clinical scenarios such as liver metastasis or head and neck cancer, multiple independent lesions appear in close proximity within a restricted anatomical volume, yet must be identified as separate entities to monitor disease progression and treatment response. Under the One-to-One rule with $\text{IoU} > 0.5$, otherwise correctly predicted segments in such regimes are systematically penalized as simultaneous *FP* and *FN*, obscuring real model improvements.

2 Related Work

The Metrics Reloaded framework recommends *PQ* for the task of instance segmentation as it fuses both detection performance and segmentation quality of successfully matched segments into a single score [20]. While the authors discuss common pitfalls, such as class imbalance, they do not offer any means to address these difficulties for instance segmentation evaluation.

Defining a fixed matching threshold to classify predictions as either *TPs* or *FPs* results in a high sensitivity to the choice of the threshold. Predicted instances just slightly below the threshold are disregarded completely and penalized harshly. Chen et al. [4] introduced sortedAP in order to completely omit a fixed threshold by instead integrating over all existing intersection thresholds. To overcome the limitation of a threshold strictly greater than 0.5, the authors propose using the Hungarian algorithm for matching, which preserves a One-to-One relationship between segments and maximizes the accumulated *IoUs* of matches.

Motivated by biased evaluation of semantic metastases segmentation towards larger instances, Jaus et al. [11] proposed Connected-Component Metrics incorporating per-component evaluation and a proximity-based matching criterion, giving each tumor the same weight irrespective of its size.

Chazalon and Carlinet [3] reformulate the matching of predicted and ground truth segments as an assignment problem on a bipartite graph in the context of historical map evaluation. They define a matching as a One-to-One relation between the disjoint vertex sets of predictions and ground truth segments, with unmatched vertices allowed on either side. The same work introduces *Normalized Panoptic Quality (NPQ)*, which integrates the F-score over matching thresholds and is argued to be an equivalent rewriting of the standard *PQ* restricted to $\tau \geq 0.5$. We adopt the bipartite formulation and extend it to sub-0.5 thresholds and different matching strategies (section 3). The relation between *NPQ*, sortedAP, and *AUTC* is discussed in section 3.5.

3 Rethinking Segment Matching for Panoptic Quality

We recast the matching of predicted to ground truth segments as a constrained bipartite assignment problem [3], preserving the behavior of standard *PQ* above $\tau = 0.5$ and admitting well-defined extensions for $\tau \leq 0.5$.

Let $G = \{g_1, \dots, g_m\}$ and $P = \{p_1, \dots, p_n\}$ denote the ground truth and predicted segments of a given class, and let $\tau \in [0, 1)$ be a matching threshold. We construct a weighted bipartite graph

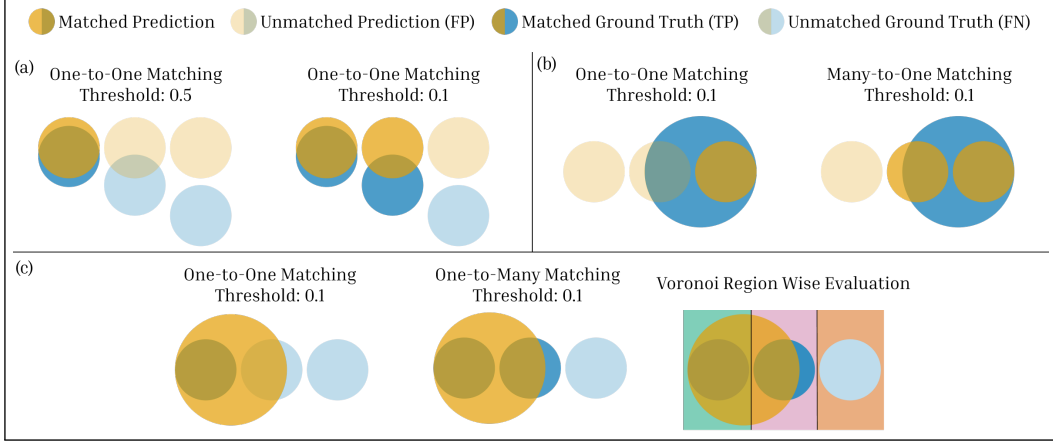


Figure 1: Comparison of different scenarios where the choice of a matching strategy and threshold impacts PQ significantly. (a) shows a scenario in which at most one predicted segment is matched to a ground truth segment and vice versa. Thus One-to-One is the appropriate matching strategy. Lowering the threshold counts the center pair as an additional TP . In scenario (b), two smaller predicted segments overlap a bigger ground truth segment: The Many-to-One matching assigns both overlapping predictions to the ground truth, resulting in a higher score. Scenario (c) shows how One-to-One matching does not credit the partial overlap of the prediction with the middle circle, whereas One-to-Many and Voronoi region-wise evaluation match the prediction with the middle circle as well.

$\mathcal{B}_\tau = (G \cup P, E_\tau, w)$ with edges

$$E_\tau = \{(g_i, p_j) \in G \times P : \text{IoU}(g_i, p_j) > \tau\} \quad (2)$$

and edge weights $w(g_i, p_j) = \text{IoU}(g_i, p_j)$. A *matching* $M \subseteq E_\tau$ is a subset of these edges. Let $\text{deg}_M(v)$ denote the number of edges in M incident to vertex v . A matching strategy is defined by independently constraining deg_M on each side of \mathcal{B}_τ to at most one or leaving it unconstrained. The first word of a strategy’s name refers to the prediction side and the second to the ground truth side: “Many-to-One” therefore means $\text{deg}_M(g)$ is unconstrained while $\text{deg}_M(p) \leq 1$, allowing multiple predicted segments to cover a single ground truth segment (fig. 1 (b)). The four resulting strategies are summarized in table 1; each is treated in detail in sections 3.1 to 3.4. The discussion of the optimization of M under each strategy is consolidated in section B.

Vertex-based TP, FP, and FN. We anchor TP and FN to ground truth vertices and FP to predicted vertices:

$$TP = \{g \in G : \text{deg}_M(g) \geq 1\}, \quad FN = \{g \in G : \text{deg}_M(g) = 0\}, \quad FP = \{p \in P : \text{deg}_M(p) = 0\}. \quad (3)$$

This is an intentional deviation from the original PQ formulation, where the one-to-one constraint makes edges and matched vertices interchangeable: each edge in M corresponds to exactly one matched ground truth and one matched predicted segment, and TP s can be identified with M itself or with the matched ground truth set. Once we relax this constraint and admit Many-to-One or One-to-Many matchings, the equivalence breaks: a single ground truth or predicted segment may be incident to multiple matched edges, and $|M|$ can exceed $|G|$ or $|P|$. We must therefore decide whether to count edges or vertices.

This vertex-centric formulation guarantees the invariant $|TP| + |FN| = |G|$ across all matching strategies, so TP and FN partition the ground truth set: every ground truth segment is either recognized or missed, never counted multiple times. *Recognition Quality* (RQ) therefore retains its interpretation as the recognition rate of ground truth segments rather than over-matching edges: a ground truth segment jointly described by several predicted segments in a Many-to-One matching contributes one TP , not several. *Segmentation Quality* (SQ) remains an average IoU per recognized object, with each ground truth segment weighted equally regardless of how many predicted segments are matched to it. The edge-based alternative $|TP| = |M|$ would violate both properties under asymmetric matchings, where $|M|$ can exceed $|G|$ or $|P|$.

Table 1: Matching strategies defined by bipartite degree constraints. The original PQ One-to-One matching constrains both predictions and ground truth segments to be part of at most one match. Many-to-One and One-to-Many each relax one constraint.

Strategy	$\deg_M(p)$	$\deg_M(g)$	Interpretation
One-to-One	≤ 1	≤ 1	Each p matches at most one g and vice versa.
Many-to-One	≤ 1		Multiple p may jointly describe one g .
One-to-Many		≤ 1	A single p may cover multiple g .
Many-to-Many			No partition structure; outside the PQ framework.

Segmentation quality under multi-edge matchings. For each matched ground truth segment $g \in TP$, let $P_M(g) = \bigcup\{p \in P : (g, p) \in M\}$ denote the union of predicted segments matched to g . We then define

$$SQ = \frac{\sum_{g \in TP} \text{IoU}(P_M(g), g)}{|TP|}, \quad (4)$$

which preserves the $[0, 1]$ bound on SQ and weights each recognized ground truth segment equally. In One-to-One and One-to-Many matchings, $P_M(g)$ is always a single predicted segment and eq. (4) reduces to the standard per-edge form. The construction is only nontrivial in the Many-to-One case (section 3.2).

3.1 One-to-One Matching

In One-to-One matching, every predicted segment matches at most one ground truth segment and vice versa. Formally, $M \subseteq E_\tau$ is a One-to-One matching if

$$\deg_M(v) \leq 1 \quad \text{for all } v \in G \cup P. \quad (5)$$

One-to-One matching credits exactly one predicted segment per ground truth segment, as depicted in fig. 1 (a). If two predicted segments both overlap the same object, only the higher- IoU one contributes to TP while the other is counted as FP (fig. 1 (b), left). Above $\tau = 0.5$, One-to-One collapses to the original PQ definition of Kirillov et al. [13].

Like standard PQ , this penalizes over- and undersegmentation symmetrically, and is the only strategy that does so. If both failure modes carry equal cost in the downstream task, only One-to-One reflects that. This approach is well-suited for scenarios in which an exact assignment of predicted to ground truth segments is non-negotiable and the ground truth annotations exhibit low ambiguity and low noise.

3.2 Many-to-One Matching

In Many-to-One matching, multiple predicted segments may jointly describe a single ground truth segment, while each predicted segment is still matched to at most one ground truth segment. Formally,

$$\deg_M(p) \leq 1 \quad \text{for all } p \in P. \quad (6)$$

Multiple predicted segments matched to a single ground truth segment are counted as a single TP , reducing the total FP count by the number of additional predicted segments absorbed into that match (fig. 1 (b)). This setting is appropriate when over-segmentation reflects a legitimate decomposition of a ground truth segment rather than a model failure, for example, when a long, thin instance is correctly recovered as several adjacent fragments.

3.3 One-to-Many Matching

In One-to-Many matching, a single predicted segment may describe multiple ground truth segments, while each ground truth segment is still matched by at most one predicted segment. Formally,

$$\deg_M(g) \leq 1 \quad \text{for all } g \in G. \quad (7)$$

This setting is appropriate when adjacent ground truth segments of the same class are difficult to delineate and a merged predicted segment should still be credited rather than penalized as both FP and FN . For example, individual cells in a dense cluster may not be separated in the predicted segment, yet still convey the correct semantic and approximate spatial extent.

3.4 Many-to-Many Matching

A Many-to-Many strategy drops degree constraints on both the prediction and ground truth sides of the bipartite graph, allowing arbitrary subsets of P to match arbitrary subsets of G . We argue that this strategy is not sensible within the Panoptic Quality framework. While our vertex-centric formulation (eq. (3)) technically preserves the $|TP| + |FN| = |G|$ invariant even here, the mathematical interpretation of these matches collapses. Specifically, a Many-to-Many assignment allows a single predicted segment to simultaneously contribute to the matched union $P_M(g)$ of multiple distinct ground truth segments in the SQ calculation (eq. (4)), double-counting predicted segments and violating the mutually exclusive nature of panoptic instances. In regimes where Many-to-Many matching is required to meaningfully evaluate a prediction, the problem is better framed as a clustering comparison rather than instance segmentation and thus operating entirely outside the bipartite assignment framework.

3.5 Area under Threshold Curve (AUTC)

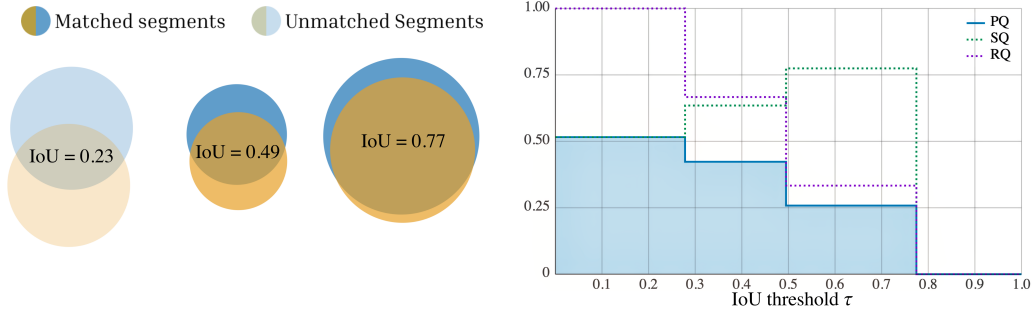


Figure 2: Left shows the One-to-One matching for the threshold $\tau = 0.49$. Right shows the step function mapping all distinct thresholds to their respective values. The *Area under Threshold Curve* reports a summary of the PQ , RQ and SQ over all thresholds. Explore this example in our interactive playground.

Choosing a fixed threshold strongly influences the evaluation by making an opinionated assumption about the minimum IoU required for a TP . And predicted segments which overlap a ground truth segment just slightly below the threshold are harshly penalized in the final PQ computation. We bypass this choice by treating τ as a free parameter and integrating PQ over all thresholds, yielding a threshold-agnostic summary. Let $PQ(\tau)$ denote the Panoptic Quality computed using the optimal matching M_τ^* derived from the thresholded bipartite graph \mathcal{B}_τ . We define the *AUTC* as

$$AUTC = \int_0^1 PQ(\tau) d\tau. \quad (8)$$

Because Panoptic Quality itself takes values in $[0,1]$ and we integrate it over the threshold parameter of unit length, *AUTC* also lies in $[0,1]$. Although defined as a continuous integral, *AUTC* reduces to an exact finite sum. Let $E_0 = \{(g_i, p_j) \in G \times P : IoU(g_i, p_j) > 0\}$ denote the edges with strictly positive overlap, and let $u_1 < u_2 < \dots < u_k$ be the unique edge weights $\{w(e) : e \in E_0\}$ in increasing order. The edge set E_τ changes only when τ crosses an element of this set, so $PQ(\tau)$ is a right-continuous step function on $[0, 1]$. Setting $u_0 = 0$, the integral becomes

$$AUTC = \sum_{i=0}^{k-1} PQ(u_i) \cdot (u_{i+1} - u_i), \quad (9)$$

where the contribution from $\tau \geq u_k$ vanishes: no edge satisfies $IoU > u_k$, so every $g \in G$ is an FN , every $p \in P$ is an FP , and $PQ(\tau) = 0$ on $[u_k, 1]$.

Decomposing *AUTC*. Both factors of PQ are themselves step functions in τ , so the same construction yields recognition- and segmentation-specific summaries:

$$AUTC_{SQ} = \int_0^1 SQ(\tau) d\tau, \quad AUTC_{RQ} = \int_0^1 RQ(\tau) d\tau, \quad (10)$$

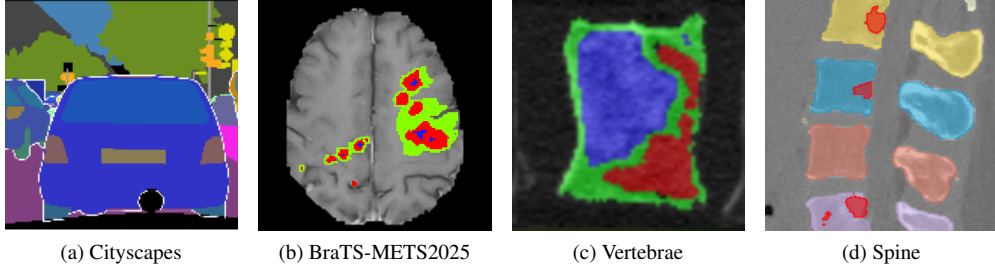


Figure 3: Examples of part-aware segmentation across domains: (a) natural-image instances with semantic parts from Cityscapes [5], (b) a BraTS-METS2025 [21] brain tumor slice showing the metastasis composed of edema (green), non-enhancing (blue), and enhancing (red) sub-regions in brain MR, (c) vertebrae highlighting healthy bone (green), lytic lesions (blue), and sclerotic lesions (red) and (d) distribution of lesions (red) across distinct vertebrae, each represented by a unique color.

both bounded in $[0, 1]$ by the same argument and computable via the discrete form of eq. (9). Reporting them alongside $AUTC$ isolates whether a method’s threshold-averaged advantage stems from better segmentation quality ($AUTC_{SQ}$) or from a higher recognition rate across thresholds ($AUTC_{RQ}$). We emphasize, however, that the multiplicative structure of PQ does *not* carry over to the integrals: in general

$$AUTC \neq AUTC_{SQ} \cdot AUTC_{RQ}, \quad (11)$$

because the integral of a product is not the product of integrals.

Relation to existing threshold-agnostic metrics. Two prior metrics also integrate a panoptic-style score over matching thresholds. Chazalon and Carlinet [3] introduce NPQ , the area under the F-score curve over $\tau \in [0, 1]$ under One-to-One matching, and argue that the standard PQ is an equivalent rewriting of NPQ at $\alpha \geq 0.5$. Chen et al. [4] propose sortedAP, which integrates the average precision score over the full threshold range using Hungarian One-to-One matching. Both metrics integrate a recognition-only score and are restricted to One-to-One matching. In contrast, $AUTC$ additionally admits Many-to-One and One-to-Many matching strategies and decomposes into $AUTC_{SQ}$ and $AUTC_{RQ}$, which isolates the source of a method’s threshold-averaged performance.

3.6 Voronoi Matching

The Voronoi variant, introduced as part of the CC-Metrics framework [22], sidesteps global bipartite matching by partitioning the image domain into per-instance cells: every voxel is assigned to its nearest ground truth segment, and predictions are scored locally inside each cell. Since each cell contains exactly one ground truth segment, the bipartite construction of section 3 reduces to $|G|$ independent intra-cell matchings, into which any of the previous strategies can be plugged. The vertex-based $TP/FN/FP$ accounting and PQ definition of eqs. (3) and (4) carry over unchanged. Predicted segments extending past a cell boundary are re-attributed to the nearest reference rather than counted as an additional FP , as depicted in fig. 1 (c). The original CC-Metrics motivation is that local averaging weights every component equally, regardless of size, preventing a few large instances from dominating the score. Embedded in our framework, the same construction additionally resolves bipartite matching ambiguity when references are dense or touching. The formal construction is given in section A.

3.7 Part-Aware Panoptic Matching

Part-aware Panoptic Quality ($PartPQ$), introduced by De Geus et al. [6], extends PQ to hierarchical targets: each scene-level class may carry an internal part decomposition, and a prediction is rewarded only if it both recovers the parent instance *and* agrees with its internal part labeling. This matches the biomedical setting almost directly: a tumor instance decomposes into edema, non-enhancing, and enhancing sub-regions; a vertebra into body, arch, and process; a cell into cytoplasm and nucleus (section 3.6).

$PartPQ$ leaves the matching machinery of PQ entirely intact: instance matching is performed exactly as in any of the strategies above on the scene-level class l , yielding the same TP , FP , and FN sets via

eq. (3). The only modification is to the *quality term*: the instance-level $\text{IoU}(P_M(g), g)$ in eq. (4) is replaced by a part-aware quantity $\text{IoU}_p(P_M(g), g)$. For a class l that carries parts ($l \in \mathcal{L}^{\text{parts}}$), IoU_p is the mean *IoU* taken over the part labels of l within the matched pair, treating voxels outside both g and p as background. For a class without parts ($l \in \mathcal{L}^{\text{no-parts}}$), it falls back to the instance *IoU*:

$$\text{IoU}_p(P_M(g), g) = \begin{cases} \text{mean IoU}_{\text{part}}(P_M(g), g), & l \in \mathcal{L}^{\text{parts}} \\ \text{IoU}_{\text{inst}}(P_M(g), g), & l \in \mathcal{L}^{\text{no-parts}}. \end{cases} \quad (12)$$

For $l \in \mathcal{L}^{\text{parts}}$, the multi-class mean is computed across all part labels of l plus the background label assigned to voxels outside the matched segments. Predictions falling on the *void* part label inside g are not counted as part-level *FPs* but are still counted as *FNs*, mirroring the convention of scene-level *PQ* [13]. Substituting IoU_p into eq. (4), the per-class PartPQ is

$$\text{PartPQ}_l = \frac{\sum_{g \in TP} \text{IoU}_p(P_M(g), g)}{|TP| + \frac{1}{2}|FP| + \frac{1}{2}|FN|}, \quad (13)$$

which preserves the $\text{SQ} \times \text{RQ}$ structure of standard *PQ* while embedding the part hierarchy into the quality numerator rather than into a separate matching pass.

Two consequences are worth highlighting. First, the hierarchy is strict: parts of an unmatched instance ($g \in FN$ or $p \in FP$) contribute nothing to the numerator of eq. (13), and are *not* separately re-matched as their own instances. A necrotic core that is correctly delineated but whose parent tumor was missed at the instance level scores as a single *FN* on the parent, not as a part-level success. This is the property that distinguishes PartPQ from the common practice of independently reporting per-region *PQ* [18]. Second, PartPQ is orthogonal to the choice of instance matcher: any of the strategies in sections 3.1 to 3.3 and 3.6 can supply the parent matching, and IoU_p is computed downstream from it. The original formulation [6] fixes this matcher to the standard One-to-One rule of Kirillov et al. [13] with $\tau = 0.5$. We relax that constraint, so the choice of matcher and the part hierarchy can be configured independently to reflect the failure modes of the underlying data.

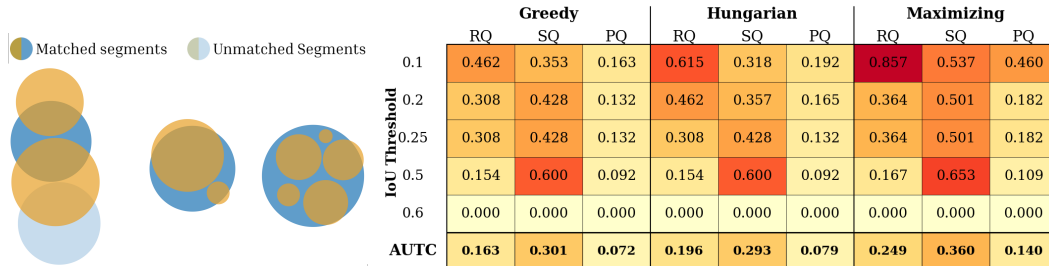


Figure 4: A toy example encompassing different scenarios in real-life segmentation tasks, like fragmented segmentation of a larger object, and the corresponding SQ, RQ, and PQ values when setting different thresholds. The left example shows a Many-to-One matching for the threshold $\tau = 0.2$. The choice of a matching strategy heavily influences all resulting metric computations as demonstrated in the table on the right. The color saturation of cells encode the reported quality. Adjust the matching strategy or the samples in our interactive playground.

4 Evaluation tutorials

We publish an interactive playground for exploring thresholds below 0.5 and different matching algorithms. The AUTC example (fig. 2) and toy example (fig. 4) may be extended and modified or completely new scenarios can be configured. Further, we provide two Jupyter notebooks showcasing the application of different strategies and part-awareness in the medical domain, including BraTS metastasis and part-aware liver lesion segmentation. All resources are accessible via an umbrella repository (<https://anonymous.4open.science/r/pq-interactive/>).

5 Discussion

We recast PQ as a constrained bipartite assignment and anchor $TP/FP/FN$ counts to vertices rather than edges, which places four well-defined matching strategies on a single design axis and preserves $|TP| + |FN| = |G|$ across all of them. On top of this, we build a threshold-agnostic summary ($AUTC$) and a part-aware extension that decouples PartPQ from the original $\text{IoU} > 0.5$ rule so the matcher and the part hierarchy can be configured independently.

The vertex-based accounting is what lets these four strategies share a metric in the first place. Under any asymmetric matching the edge count $|M|$ can exceed $|G|$ or $|P|$. Identifying TP s with edges would push RQ above 1 and dissolve its interpretation as a recognition rate. Anchoring TP and FN to ground-truth vertices closes this gap, so RQ stays directly comparable across One-to-One, Many-to-One, and One-to-Many matchings.

Across the toy example and case studies, the choice of strategy maps onto a tension between RQ and SQ . One-to-One enforces a strict per-object assignment and is the only strategy that penalizes over- and undersegmentation symmetrically. The max-weight greedy variant of Kofler et al. [14] occasionally trades a marginal recognition for a higher accumulated overlap when two predictions cover the same reference, but in practice the two coincide in the vast majority of cases. Many-to-One greedy merge is the most lenient strategy under fragmentation, yet it still requires a single edge above τ to register a detection: in the toy example, this produces a sharp drop above $\tau \approx 0.2$ even when accumulated overlap across the reference remains high, so a heavily fragmented prediction can still be counted as a FN . Reporting $AUTC$ bypasses the dependence on a single threshold, and its decomposition into $AUTC_{SQ}$ and $AUTC_{RQ}$ isolates whether a method’s threshold-averaged advantage comes from better localisation or higher recognition.

Choosing among the strategies is therefore less a question of correctness than of which failure modes the downstream task treats as recoverable. One-to-One is the safe default when annotations are clean, instances are well-separated, and a strict per-instance assignment is non-negotiable. Many-to-One fits regimes in which over-segmentation reflects a legitimate decomposition rather than a model failure. One-to-Many is the right tool when adjacent same-class instances are inherently hard to delineate and a merged prediction should still convey the correct semantic and approximate spatial extent. One-to-Many matching remains the most opinionated point in this design space. Crediting a single prediction for several reference segments tolerates undersegmentation in a way that fundamentally rebalances SQ against RQ , and the appropriate behavior depends on whether the downstream task treats a merged object as recoverable or as a hard failure.

The interaction between matcher and part hierarchy is most consequential under Many-to-One. When several adjacent fragments are credited as a single parent instance, their union defines the part-level IoU_p , so a fragmented prediction whose parts are individually correct can recover full part-level credit, whereas the original One-to-One rule of De Geus et al. [6] would reject the whole instance and discard its part labeling along with it.

Limitations, future work, and conclusion. Many-to-Many matching is intentionally outside our framework because the bipartite formulation breaks down once both degree constraints are dropped. Related approaches such as Cluster Dice [17] address the same failure mode through clustering, and a unified treatment that bridges assignment and clustering views remains open. The suggested greedy merge for Many-to-One is an approximation without an established optimality guarantee against M_{PQ}^* (section B). Tighter algorithmic bounds or an exact tractable reformulation would put the strategy on firmer ground. Our empirical study is limited in scope: we cover a small number of cases and a single model family per task, with PartPQ evaluated only on biomedical data and threshold-sensitivity analyses run on a subset of the benchmarks, so a larger-scale comparison spanning natural-image datasets, additional architectures, and the full strategy \times threshold grid is the most pressing direction for follow-up work.

We present a unified framework for PQ below the standard $\text{IoU} > 0.5$ threshold, recasting segment matching as a constrained bipartite assignment in which vertex-based accounting keeps PQ consistent across One-to-One, Many-to-One, One-to-Many, and Voronoi matchings. The four strategies form a small, well-defined design space, and the right choice is set by which failure modes the downstream task treats as recoverable rather than by a single default. We release the framework as a unified open-source package built on Panoptica, so practitioners can configure the matcher, threshold, and part hierarchy to match their data.

References

- [1] Pedro R. A. S. Bassi, Mehmet Can Yavuz, Kang Wang, Xiaoxi Chen, Wenxuan Li, Sergio Decherchi, Andrea Cavalli, Yang Yang, Alan Yuille, and Zongwei Zhou. Radgpt: Constructing 3d image-text tumor datasets, 2025. URL <https://arxiv.org/abs/2501.04678>.
- [2] Patrick Bilic, Patrick Christ, Hongwei Bran Li, Eugene Vorontsov, Avi Ben-Cohen, Georgios Kaissis, Adi Szeskin, Colin Jacobs, Gabriel Efrain Humpire Mamani, Gabriel Chartrand, et al. The liver tumor segmentation benchmark (lits). *Medical image analysis*, 84:102680, 2023.
- [3] Joseph Chazalon and Edwin Carlinet. Revisiting the Coco Panoptic Metric to Enable Visual and Qualitative Analysis of Historical Map Instance Segmentation. In Josep Lladós, Daniel Lopresti, and Seiichi Uchida, editors, *16th International Conference on Document Analysis and Recognition, IC-DAR 2021, Lausanne, Switzerland, September 5-10, 2021, Proceedings, Part IV*, Lecture Notes in Computer Science, pages 367–382. Springer. doi: 10.1007/978-3-030-86337-1_25. URL https://doi.org/10.1007/978-3-030-86337-1_25.
- [4] Long Chen, Yuli Wu, Johannes Stegmaier, and Dorit Merhof. Sortedap: rethinking evaluation metrics for instance segmentation. In *Proceedings of the IEEE/CVF international conference on computer vision*, pages 3923–3929, 2023.
- [5] Marius Cordts, Mohamed Omran, Sebastian Ramos, Timo Rehfeld, Markus Enzweiler, Rodrigo Benenson, Uwe Franke, Stefan Roth, and Bernt Schiele. The cityscapes dataset for semantic urban scene understanding. In *Proceedings of the IEEE conference on computer vision and pattern recognition*, pages 3213–3223, 2016.
- [6] Daan De Geus, Panagiotis Meletis, Chenyang Lu, Xiaoxiao Wen, and Gijs Dubbelman. Part-aware panoptic segmentation. In *Proceedings of the IEEE/CVF Conference on Computer Vision and Pattern Recognition*, pages 5485–5494, 2021.
- [7] Adrien Foucart, Olivier Debeir, and Christine Decaestecker. Panoptic quality should be avoided as a metric for assessing cell nuclei segmentation and classification in digital pathology. *Scientific reports*, 13(1):8614, 2023.
- [8] Bharath Hariharan, Pablo Andrés Arbeláez, Ross B. Girshick, and Jitendra Malik. Simultaneous detection and segmentation. In David J. Fleet, Tomás Pajdla, Bernt Schiele, and Tinne Tuytelaars, editors, *Computer Vision - ECCV 2014 - 13th European Conference, Zurich, Switzerland, September 6-12, 2014, Proceedings, Part VII*, Lecture Notes in Computer Science, pages 297–312. Springer, 2014. doi: 10.1007/978-3-319-10584-0_20. URL https://doi.org/10.1007/978-3-319-10584-0_20.
- [9] Kaiming He, Georgia Gkioxari, Piotr Dollár, and Ross B. Girshick. Mask R-CNN. *CoRR*, abs/1703.06870, 2017. URL <http://arxiv.org/abs/1703.06870>.
- [10] Nicholas Heller, Fabian Isensee, Klaus H Maier-Hein, Xiaoshuai Hou, Chunmei Xie, Fengyi Li, Yang Nan, Guangrui Mu, Zhiyong Lin, Miofei Han, et al. The state of the art in kidney and kidney tumor segmentation in contrast-enhanced ct imaging: Results of the kits19 challenge. *Medical image analysis*, 67:101821, 2021.
- [11] Alexander Jaus, Constantin Marc Seibold, Simon Reiß, Zdravko Marinov, Keyi Li, Zeling Ye, Stefan Krieg, Jens Kleesiek, and Rainer Stiefelhagen. Every component counts: rethinking the measure of success for medical semantic segmentation in multi-instance segmentation tasks. In *Proceedings of the AAAI Conference on Artificial Intelligence*, volume 39, pages 3904–3912, 2025.
- [12] Doris Kaltenecker, Rami Al-Maskari, Moritz Negwer, Luciano Hoehner, Florian Kofler, Shan Zhao, Mihail Todorov, Zhouyi Rong, Johannes Christian Paetzold, Benedikt Wiestler, et al. Virtual reality-empowered deep-learning analysis of brain cells. *Nature Methods*, 21(7):1306–1315, 2024.
- [13] Alexander Kirillov, Kaiming He, Ross Girshick, Carsten Rother, and Piotr Dollár. Panoptic segmentation. In *Proceedings of the IEEE/CVF conference on computer vision and pattern recognition*, pages 9404–9413, 2019.
- [14] Florian Kofler, Hendrik Möller, Josef A Buchner, Ezequiel de la Rosa, Ivan Ezhov, Marcel Rosier, Isra Mekki, Suprosanna Shit, Moritz Negwer, Rami Al-Maskari, et al. Panoptica—instance-wise evaluation of 3d semantic and instance segmentation maps. *arXiv preprint arXiv:2312.02608*, 2023.
- [15] Florian Kofler, Suprosanna Shit, Ivan Ezhov, Lucas Fidon, Izabela Horvath, Rami Al-Maskari, Hongwei Bran Li, Harsharan Bhatia, Timo Loehr, Marie Piraud, et al. Blob loss: Instance imbalance aware loss functions for semantic segmentation. In *International Conference on Information Processing in Medical Imaging*, pages 755–767. Springer, 2023.
- [16] H. W. Kuhn. The hungarian method for the assignment problem. *Naval Research Logistics Quarterly*, 2(1-2):83–97, 1955.

- [17] Soumya Snigdha Kundu, Aaron Kujawa, Marina Ivory, Theodore Barfoot, Jonathan Shapey, and Tom Vercauteren. Cluster dice: a simple and fast approach for instance-based semantic segmentation evaluation via many-to-many matching. In *Medical Imaging 2025: Computer-Aided Diagnosis*, volume 13407, pages 226–232. SPIE, 2025.
- [18] Dominic LaBella, Katherine Schumacher, Michael Mix, Kevin Leu, Shan McBurney-Lin, et al. Brain tumor segmentation (BraTS) challenge 2024: Meningioma radiotherapy planning automated segmentation. *arXiv preprint arXiv:2405.18383*, 2024.
- [19] Jonathan Long, Evan Shelhamer, and Trevor Darrell. Fully Convolutional Networks for Semantic Segmentation. abs/1411.4038. URL <http://arxiv.org/abs/1411.4038>.
- [20] Lena Maier-Hein, Annika Reinke, Patrick Godau, Minu D Tizabi, Florian Buettner, Evangelia Christodoulou, Ben Glocker, Fabian Isensee, Jens Kleesiek, Michal Kozubek, et al. Metrics reloaded: recommendations for image analysis validation. *Nature methods*, 21(2):195–212, 2024.
- [21] Nazanin Maleki, Raisa Amiruddin, Ahmed W Moawad, Nikolay Yordanov, Athanasios Gkampenis, Pascal Fehringer, Fabian Umeh, Crystal Chukwurah, Fatima Memon, Bojan Petrovic, et al. Analysis of the miccai brain tumor segmentation–metastases (brats-mets) 2025 lighthouse challenge: Brain metastasis segmentation on pre-and post-treatment mri. *arXiv preprint arXiv:2504.12527*, 2025.
- [22] Pierre Rougé, Odyssee Merveille, and Nicolas Passat. ccDice: A topology-aware Dice score based on connected components. In *Topology- and Graph-Informed Imaging Informatics: First International Workshop, TGI3 2024, Held in Conjunction with MICCAI 2024*, Lecture Notes in Computer Science, pages 11–21. Springer, 2024. doi: 10.1007/978-3-031-73967-5_2.
- [23] Felix Sigmund, Oleksandr Berezin, Sofia Beliakova, Bernhard Magerl, Martin Drawitsch, Alberto Piovesan, Filipa Gonçalves, Silviu-Vasile Bodea, Stefanie Winkler, Zoe Bousraou, et al. Genetically programmable barcodes for correlative volume electron microscopy. *2023 Synthetic Biology: Engineering, Evolution & Design (SEED)*, 2023.
- [24] C. J. van Rijsbergen. *Information Retrieval*. Butterworth, 1979. ISBN 0-408-70929-4.

Appendix

A Voronoi Matching: Formal Construction

Let Ω denote the image domain and $d(x, g)$ the (Euclidean) distance from voxel $x \in \Omega$ to the nearest voxel of ground truth segment $g \in G$. The Voronoi cell of g is

$$V(g) = \{x \in \Omega : d(x, g) \leq d(x, g') \quad \forall g' \in G\}, \quad (14)$$

with ties broken arbitrarily so that $\{V(g)\}_{g \in G}$ partitions Ω . For each ground truth segment we define its *local prediction* as the restriction of all predicted segments to its cell,

$$\tilde{p}(g) = \left(\bigcup_{p \in P} p \right) \cap V(g), \quad (15)$$

and replace the bipartite edge set of eq. (2) with the per-cell edges

$$E_\tau^{\text{Vor}} = \{(g, \tilde{p}(g)) : g \in G, \text{IoU}(g, \tilde{p}(g)) > \tau\}. \quad (16)$$

The resulting matching $M^{\text{Vor}} = E_\tau^{\text{Vor}}$ is one-to-one by construction—each ground truth segment is paired with the unique aggregated prediction inside its cell—so the *TP/FN/FP* accounting of eq. (3) and the *SQ/RQ/PQ* definitions of eq. (4) apply unchanged. Predicted mass that falls outside every cell never contributes to a *TP* but is still penalised through the global *FP* count.

The construction generalises directly: rather than aggregating all predictions inside a cell into a single $\tilde{p}(g)$, the chosen instance matcher (One-to-One, Many-to-One, or One-to-Many) can be applied independently within each cell, and the per-cell results are aggregated into the global *TP/FN/FP* counts. This is the form realised by Panoptica’s region-wise pipeline, in which a Voronoi partition is computed once on the reference and the standard bipartite matching is run inside every cell.

B Optimal Matching Across Strategies

A matching strategy constrains the structure of M but does not pin it down: multiple matchings may satisfy a strategy’s degree constraints. We must therefore specify an objective that selects an optimal matching M^* . Since *PQ* is the metric we ultimately report, the principled choice is to optimise it directly,

$$M_{\text{PQ}}^* = \arg \max_M \text{PQ}(M). \quad (17)$$

PQ couples edges through the union $P_M(g)$ in the *SQ* numerator and through the global $|TP|, |FP|, |FN|$ counts in the *RQ* denominator, so it does not decompose into a sum over edges and admits no obvious polynomial algorithm.

We therefore work with an edge-decomposable surrogate, the *max-weight matching*

$$M_{\text{weight}}^* = \arg \max_M \sum_{(g,p) \in M} \text{IoU}(g, p), \quad (18)$$

and ask, for each strategy, whether M_{weight}^* coincides with M_{PQ}^* exactly, whether it diverges from M_{PQ}^* and must be replaced by an approximation that lower-bounds $\text{PQ}(M_{\text{PQ}}^*)$, or whether the matching is uniquely determined by construction.

One-to-One. Under the one-to-one constraint, $M_{\text{weight}}^* = M_{\text{PQ}}^*$ exactly. Every matched ground truth has $|P_M(g)| = 1$, so the *SQ* numerator equals the edge-weight sum, and $|TP| = |M|$, $|FP| = |P| - |M|$, $|FN| = |G| - |M|$ make the *PQ* denominator $\frac{1}{2}(|G| + |P|)$ independent of M . Hence *PQ* is monotone in the edge-weight sum, and

$$M^* = \arg \max_{M \text{ one-to-one}} \sum_{(g,p) \in M} \text{IoU}(g, p) \quad (19)$$

solves (17) exactly. M^* is computable in $O((m+n)^3)$ time by the Hungarian algorithm [16]. For $\tau > 0.5$, the unique-matching property of Kirillov et al. [13, Theorem 1] guarantees that any consistent assignment returns the same M^* , and our formulation reduces to the original *PQ* matching. For $\tau \leq 0.5$ Hungarian assignment is required since the constraint is no longer automatically satisfied as multiple ground truths can compete for the same predicted segment.

Many-to-One. Many-to-One is the only strategy in which the surrogate provably diverges from max- PQ : absorbing a low-overlap predicted segment into an already well-covered ground truth can increase the edge-weight sum while decreasing $\text{IoU}(g, P_M(g))$, so M_{weight}^* may dilute SQ relative to M_{PQ}^* . We therefore drop the proxy and target the SQ contribution per ground truth directly. Finding M_{PQ}^* exactly under this constraint is, to our knowledge, intractable in general, so we adopt an approximation: algorithms that admit a candidate prediction only when it strictly improves the combined overlap, such as the greedy merge of Kofler et al. [14], avoid the dilution failure mode and yield a valid matching whose PQ is a lower bound on $PQ(M_{PQ}^*)$.

One-to-Many. Because $\text{deg}_M(g) \leq 1$, each $g \in TP$ has $|P_M(g)| = 1$, and the SQ numerator again equals the edge-weight sum. Moreover, ground truth segments do not compete for predicted segments: a single predicted segment may match arbitrarily many ground truth segments. The max-weight matching therefore reduces to selecting, independently for each ground truth segment, its highest-IoU predicted segment above τ (or no edge at all):

$$M^* = \bigcup_{g \in G} \{(g, \arg \max_{p: \text{IoU}(g,p) > \tau} \text{IoU}(g,p))\}, \quad (20)$$

which is computable in $O(mn)$ time. Max-weight remains our default objective: it coincides with max- PQ whenever $\tau \geq 0.5$ and differs from it only for low-IoU edges that would barely satisfy the threshold while diluting the SQ average.

Voronoi. No optimisation is required: the partition $\{V(g)\}$ depends only on the ground truth, not on P , so M^{Vor} is uniquely determined and trivially optimal under its own definition. Constructing the cells reduces to a single distance transform on G , computable in $O(|\Omega|)$ time, after which each per-cell IoU is evaluated in time linear in $|V(g)|$.

Part-Aware. PartPQ does not introduce a new optimisation problem. The parent matching M^* is computed by the optimiser of the chosen instance strategy (eqs. (19) and (20), the greedy merge above for Many-to-One, or the deterministic Voronoi partition of section 3.6); IoU_p is then evaluated per matched pair in time linear in the matched volume. Optimising the parent matching for PartPQ rather than for the scene-level PQ would couple part- and instance-level overlaps and is, to our knowledge, not addressed in the literature; we treat the parent-then-parts decomposition as the operational definition.

C Figures

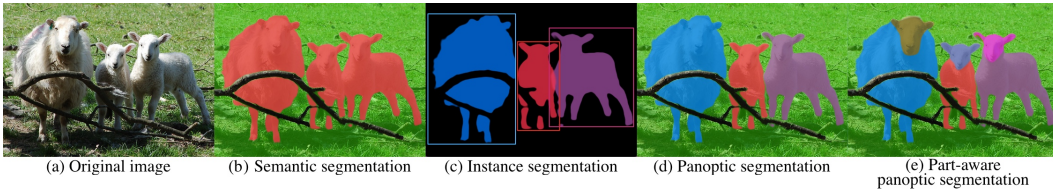


Figure 5: Semantic segmentation delineates *stuff* (grass and sheeps) exclusively (b), whereas panoptic segmentation augments semantic classes with *things* which are countable objects like individual sheeps (d). Instance segmentation permits multiple instance assignments per pixel in contrast to panoptic segmentation (c). Part-aware panoptic segmentation combines scene and part parsing in a single task (e).